Bandgap extraction from quantum efficiency spectra of Cu(In,Ga)Se$_2$ solar cells with varied grading profile and diffusion length

M Richter *, MS. Hammer, T Sonnet, J Parisi

Laboratory for Chalcogenide Photovoltaics, Energy and Semiconductor Research Laboratory, Department of Physics, University of Oldenburg, 26111 Oldenburg, Germany

ABSTRACT

Quantum efficiency measurements on Cu(In,Ga)Se$_2$ (CIGS) solar cells are widely used as a non-destructive and easy to apply method to extract the bandgap of the CIGS absorber layer. Information about the bandgap is of major relevance, e.g., for process control or parameter definition in device simulations. However, determining the bandgap from quantum efficiency measurements rely on the assumption that the quantum efficiency is solely determined by the absorption of a homogeneous absorber layer. We therefore compared different bandgap extraction models while taking into account different bandgap grading profiles and diffusion lengths, thus different bulk recombination properties. To study the effects of limited diffusion and grading in more detail, we created a one-dimensional optical simulation tool that calculates the optics by means of the generalized transfer matrix method. The tool includes models to account for roughness, thickness non-uniformity and graded layers. By fitting the model to the measured external quantum efficiency (EQE), we determine the bandgap gradient, which is compared to that calculated from the composition measured with glow discharge optical emission spectroscopy. We found that common methods to extract the bandgap overestimate the band gap value from EQE by up to 150 meV depending on the slope of the grading. In contrast to this, the influence of the diffusion length on the extracted bandgap is negligible.

© 2016 Elsevier B.V. All rights reserved.

1. Introduction

External quantum efficiency (EQE) measurements of solar cells provide detailed information about the spectral optical and electrical loss mechanisms that determine the maximum current the solar cell can provide. Optical losses comprise parasitic absorption in functional layers, transmission in absorber layers and reflection at the surface as well as at internal interfaces. Additionally, a limited collection probability for generated minority carriers due to recombination reduces the EQE. The transmission in the absorber layer is determined by the bandgap, which therefore could be extracted from EQE measurements by different methods [1–3]. In contrast, the direct transmission measurement of the absorber layer prepared on a transparent substrate is often not reliable since the processing is different. Nevertheless, a precise knowledge of the absorber bandgap is of high relevance for assessing the potential open-circuit voltage or the input parameters for electrical device simulations [4–6].

Looking at thin-film solar cells, coherent light interferences could cause local field enhancements and especially those solar cells based on Cu(In$_{1-x}$,Ga$_x$)Se$_2$ (CIGS) could additionally exhibit a depth-graded composition (and hence bandgap grading). These features make

interpretation of EQE measurements complicated. As many factors determine the EQE, a simulation is an appropriate method to investigate the different loss mechanism in more detail. We created an easy-to-use optical simulation tool with graphical user interface [7] to perform coherent, incoherent, and partly coherent/incoherent optical simulations of an arbitrary one-dimensional stack of thin and/or thick layers. Furthermore, a user defined composition grading and collection function could be used to calculate the local generation rate and EQE. As input parameters for the optical simulation the layer thicknesses, optical constants (spectral and composition dependent), and – in case of roughness – the roughness height and/or Haze value should be known. For the electrical part, the diffusion constant, diffusion length, and surface recombination velocity are required. The output contains on the one hand the spectrally resolved reflection, transmission, and total and layer-wise absorption and on the other hand, the depth resolved field distribution, optical generation rate, and collected carrier density that yields the EQE.

For this study, we used this tool to obtain the composition gradient and diffusion length of CIGS solar cells with varied grading profiles and compare the gradients with glow-discharge optical emission spectroscopy (GDOES) analysis. The metastability of the CIGS allows changing the space charge region width and diffusion length by light-soaking [8]. By this, a validation of the simulation model is possible. Furthermore, this paper discusses the influence of different grading profiles

* Corresponding author.
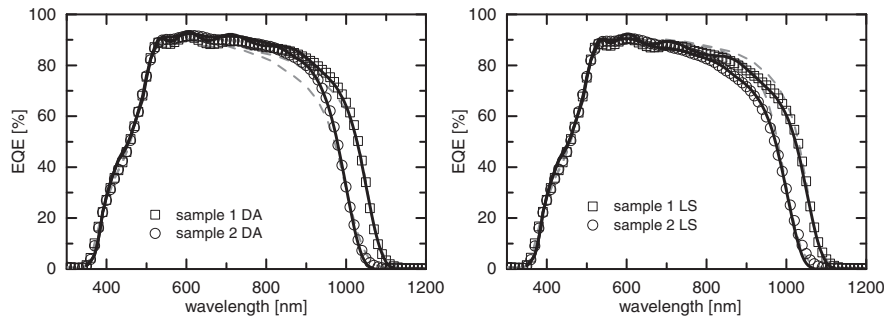*E-mail address:* michael.richter@uni-oldenburg.de (M. Richter).

Fig. 1. EQE of two samples with different gallium content (symbols) and respective simulation results (solid lines). On the left, the DA state is considered while for comparison, dashed lines indicate the LS measurement. Vice versa on the right for the LS state.

and diffusion lengths on the effective bandgap for absorption and photocurrent collection assessed by different extraction methods to evaluate their accuracy in giving the real minimum bandgap value of the absorber.

2. Experimental details

The samples were derived from state-of-the-art glass/Mo/Cu(In$_{x-1}$,Ga$_x$)Se$_2$/CdS/i-ZnO/ZnO:Al solar cells. The CIGS absorber was manufactured by a co-evaporation multistage process. The optical constants refractive index n and extinction coefficient k of Mo, CdS, i-ZnO, and ZnO:Al layers were determined with a Woollam VASE ellipsometer [9], whereby n and k from CIGS were taken from [10]. The EQE was measured with a commercial Bentham PVE300 with an integrating sphere for measurement of the total and diffuse reflection. All samples were measured at dark annealed (DA) state (relaxed at 90 °C for 9 h in dark) and at light soaked (LS) state (annealed at 90 °C for 9 h at 1 sun). Capacitance voltage measurements were done to determine the space charge region width that changes between DA and LS states [8]. For thickness measurements, a FEI scanning electron microscope was applied. A Spectruma Analytik GDA 750 system was used to perform GDOES. The elemental concentrations allow the calculation of the bandgap. The mole fraction ratio $GGI = Ga/(Ga + In)$ changes the bandgap of CIGS by [11]

$$E_g(GGI) = (1-GGI)E_{g,CIS} + GGI \cdot E_{g,CGS} + b \cdot GGI(1-GGI) \qquad (1)$$

with $E_{g,CIS}$ and $E_{g,CGS}$ as bandgap values for pure CuInSe$_2$ and CuGaSe$_2$, respectively. The values of the optical bowing constant b as well as those of $E_{g,CIS}$ and $E_{g,CGS}$ are discussed in the literature [12–15] while we assume $b = 0.13$, $E_{g,CIS} = 1.04$ eV, and $E_{g,CGS} = 1.68$ eV. Furthermore, we are not considering a possible change in bandgap due to Cu variation [16].

To extract the bandgap from an EQE spectrum, three different methods were applied. Gärtner [17] proposed a model for the total photocurrent that gives

$$IQE(\lambda) = 1 - \frac{\exp(-\alpha W)}{1 + \alpha L} \qquad (2)$$

for the internal quantum efficiency IQE, with λ, α, W, and L as wavelength, absorption coefficient, space charge region width and minority carrier diffusion length, respectively. At bandgap energies and limited diffusion $\alpha \cdot L$ could be neglected and we get

$$IQE(\lambda) \approx 1 - \exp(-\alpha W) \qquad (3)$$

The relationship of α and the bandgap E_g for direct transitions is given by [18]

$$\alpha = \frac{A}{E_{ph}}(E_{ph}-E_g)^{1/2} \qquad (4)$$

where A is the constant for fundamental absorption which is set to $5 \cdot 10^4$ cm^{-1} eV$^{-1/2}$ and E_{ph} is photon energy. Combining Eqs. (2) and (4) and assuming a constant reflection and parasitic absorption at energies near the bandgap, we arrive at the relation

$$(E_{ph} \cdot EQE)^2 \propto E_{ph} - E_g \qquad (5)$$

that holds for low EQE values or at the more general relation:

$$[E_{ph} \cdot \ln(1-EQE)]^2 \propto E_{ph} - E_g \qquad (6)$$

Eqs. (5) and (6) require a constant α throughout the depth, which is generally not the case for composition graded layers. Troviano and Taretto [19] developed a model to account for a linearly graded absorber layer and for Urbach band tail absorption. The latter exhibits exponential behavior [20], thus the relationship is as follows

$$\left[-\ln(1-EQE) - \frac{2A E_u^{3/2}}{3\beta \sqrt{2}}\right]^{2/3} \propto E_{ph} - E_g \qquad (7)$$

with the grading parameter $\beta = (E_{g,back} - E_{g,front})/d$, where d is absorber thickness, and E_u as Urbach band-tail energy.

Plotting the left side of Eqs. (5)–(7) versus E_{ph} allows a linear fit with the effective bandgap E_g as x-axis intercept. We refer Eqs. (5)–(7) in the following to as method A, B, and C. Other bandgap extraction methods like taking the energy at the maximum derivative of the EQE [21] or assuming the energy at a distinct value of EQE [22] are not considered here.

3. Optical modeling

The calculation of the device optics is based on the generalized transfer matrix method (GTMM) [23,24] that accounts for light propagation in coherent and incoherent layers by treating both with a system of interface and layer transition matrices. In case of an incoherent layer the electrical field intensity is used instead of electrical field amplitude. This method allows for calculating the total reflection, transmission as well as local time-averaged power dissipation, and hence generation

Table 1
Simulation parameters (*italic*) gained from fitting to EQE measurements of two different samples at dark annealed (DA) and light soaked (LS) state. Space charge region width W is determined with capacitance voltage measurements. Short circuit current density is calculated by $J_{sc} = q\int EQE \cdot \Phi_0(\lambda)\, d\lambda$ with photon flux of the AM1.5 g solar spectrum.

		W [nm]	L [nm]	$E_{g,front}$ [eV]	$E_{g,back}$ [eV]	β [meV/μm]	$J_{sc,measured}$ [mA/cm^2]	$J_{sc,simulated}$ [mA/cm^2]
Sample 1	DA	643	*1050*	*1.144*	*1.253*	*54*	31.423	32.100
	LS	289	*1145*	*1.144*	*1.253*	*54*	30.703	31.198
Sample 2	DA	601	*1195*	*1.193*	*1.340*	*73*	29.50	30.127
	LS	220	*900*	*1.193*	*1.340*	*73*	28.448	28.750